CFSRC COLLOQUIUM

Proceedings of the Cold-Formed Steel Research Consortium Colloquium
17-19 October 2022 (cfsrc.org)

Moment capacity of cold-formed steel channel beams with edge-stiffened holes by machine learning

Yecheng Dai[1], Krishanu Roy[2], Zhiyuan Fang[3], Gary M. Raftery[4], James B.P. Lim[5]

Abstract

A novel machine learning model, eXtreme Gradient Boosting (XGBoost), was used for the purpose of predicting the moment capacity of cold-formed steel (CFS) channel beams with edge-stiffened web holes subject to bending. A total of 1,620 data points were generated for training the XGBoost model, using an elasto-plastic finite element model which was validated against 12 sets of test data taken from the literature. The R^2 score of XGBoost predictions for the moment capacity was around 99%. The performance of current design equations was evaluated through the comparison of their results against those obtained from the XGBoost model. The moment capacities obtained from the XGBoost testing dataset were also compared with that obtained from the existing design equations for un-stiffened holes (USH) and edge-stiffened holes (ESH). The moment capacities determined from the current design equations for USH and ESH were found to be excessively conservative by 38.3%, and unconservative by 36.2% on average, respectively. Therefore, new design equations were proposed based on the results of parametric study using the XGBoost model. From the results of XGBoost outputs, the absolute percentage error of new design equations for that based on the strengths of plain CFSCB was 8.78%, and for that based on the strengths of CFSCB with USH, the absolute percentage error was 13.7%. Additionally, a reliability analysis was performed to evaluate the accuracy of the proposed equations in predicting the moment capacity of CFS channel beams with ESH subject to bending. The reliability indices of all the proposed equations were greater than 2.5 which can be reliable as per the guidelines of AISI.

1. Introduction

The use of cold-formed steel (CFS) members in structural engineering is increasing because of their high strength to weight ratio and for ease of installation [1-3]. CFS channel beams (CFSCB) have been used as major load-bearing members in engineering applications. These beams usually have holes that are perforated on the web to accommodate plumbing and heating services, and such web holes are often un-stiffened. The spacing and dimensions of un-stiffened holes (USH) are generally limited as they impact directly on the moment capacity of such CFSCB with USH. In recent times, a new generation of CFSCB with edge-stiffened holes (ESH) (Figure. 1) designed by Howick Ltd. [4] have been widely used in New Zealand. However, current design standards such as the American Iron and Steel Institute (AISI) [5] and the Australian and New Zealand Standards (AS/NZS) [6] do not provide guidance for predicting the moment capacity of such CFSCB with ESH. Only Yu [7] proposed a design equation to calculate the moment capacity of CFSCB, but Yu's [7] equation was for CFSCB failing only in local buckling failure mode, without considering other buckling failure modes. Furthermore, no test data was used to validate Yu's equation. More importantly, the equations for lateral-torsional buckling as well as distortional buckling of CFSCB with ESH were not addressed [7].

Limited research has been conducted with regards to CFSCB with ESH subject to various loading conditions. Concerning the studies on the bending behaviour of CFSCB with ESH, Yu [6]7 numerically investigated the influence of ESH on the moment capacity of CFSCB. The moment capacity was seen to improve by 14% on average in comparison with that of a channel section having a plain web. Experimental investigations were carried out on the cold-formed steel (CFS) single channel beams with ESH [8] and on CFS back-to-back channel beams with ESH [9], respectively. In terms of the compression behaviour of CFSCB with ESH, Chen et al. [10-12] and Chi et al. [13] carried out experimental and numerical investigations on the behaviour of such CFS stiffened channels subject to axial force. It was revealed that the compression capacity of CFSCB with ESH was higher than that with a plain web. Based on the outcomes reported by Chen et al. [10-12], extensive studies were presented by Fang et al. [14] with the

[1] Ph.D. student, Department of Civil and Environmental Engineering, The University of Auckland, ydai151@aucklanduni.ac.nz
[2] Senior lecturer, School of Engineering, The University of Waikato, krishanu.roy@waikato.ac.nz
[3] Post-doctoral fellow, School of Engineering, The University of Waikato, afang@waikato.ac.nz
[4] Senior lecturer, Department of Civil and Environmental Engineering, The University of Auckland, g.raftery@auckland.ac.nz
[5] Professor, School of Engineering, The University of Waikato, James.Lim@waikato.ac.nz

application of a deep belief network (DBN) trained by around 50,000 data points to obtain the compression capacity of CFS channel columns with ESH. These data points were generated from elasto-plastic FE models which incorporated residual stresses and initial geometric imperfections [14]. Regarding the web crippling behavior, the bearing capacity of CFSCB with ESH was demonstrated to be almost as much as that of CFSCB with a plain web, both subject to One-Flange loading [15] and Two-Flange loading [16-18]. In relation to the shear behavior, experimental research was performed by Chen et al [19] to study the shear behavior of CFSCB with ESH. The results of CFSCB with USH obtained from the AISI [5] and AS/NZS [6] were found to be unconservative by 7% in comparison with that of CFSCB with ESH. Kanthasamy et al. [20] numerically validated the test results of Chen et al. [8], and then carried out parametric studies to investigate the shear capacity of doubly symmetric beams having circular ESH. The edge-stiffener length was recommended to be set as 15 mm and modified design equations were proposed over the existing Direct Strength Method (DSM) design rules.

Machine learning (ML) is a useful tool for identifying useful data features [21]. There has been a recent rise in interest to apply data-driven or ML approaches to estimate the complex underlying relationships [22]. XGBoost is an efficient machine learning method developed by Chen and Guestrin [23]. The main advantage of XGBoost in comparison with the standard machine learning algorithms is the faster computational capacity. Chen and Guestrin [23] found that the computational end-to-end costs including data loading can be ten times lesser than other machine learning methods in general when using 1.7 billion examples. The second advantage of XGBoost compared to other machine learning methods is the higher accuracy. To investigate the accuracy of different machine learning methods, Fang et al. [12] and Degtyarev and Tsavdaridis [24] evaluated the performance perforated steel beams using various machine learning methods, comprising DBN, XGBoost, Decision Tree, Random Forest, K-Nearest Neighbors, LightGBM and CatBoost. It was proven that XGBoost provided the best prediction results for both training and testing datasets.

Previous research mainly used experimental tests, finite element analysis (FEA), and some basic machine learning algorithms to study the behaviors of perforated CFS members. Compared to FEA, machine learning method is faster and more convenient. This study aims to provide a new XGBoost framework that can predict the moment capacity of CFSCB with ESH. Additionally, the current design standards don't include any guidance for determining the moment capacity of CFSCB with ESH. As a result, new design equations were proposed. A nonlinear elasto-plastic FE model was first developed and then validated with the test data available in the literature. To train the XGBoost model, a total of 1,620 data points were acquired based on the validated FE model. The test data was divided into two parts: input data and output data. ML models comprising XGBoost and Linear Regression were then utilized to predict the results and to obtain the absolute percentage errors so that the accuracy of the various techniques could be determined. When XGBoost predictions were compared with the moment capacity of stiffened CFSCB calculated as per the AISI [18], AS/NZS [19] and Yu [6], the XGBoost model was found to perform better than the current design equations. The influences of various parameters on the moment capacity of CFSCB with ESH were also investigated. Furthermore, design equations used for the prediction of the moment capacity of CFSCB with ESH subject to bending were proposed using the data obtained from the XGBoost model. Finally, a reliability analysis was performed to evaluate the reliability of the proposed design equations for predicting the moment capacity of cold-formed steel channel beams with edge stiffened web holes.

2. Summary of test results reported by Chen et al. [13]

Chen et al. [8] tested the behavior of CFSCB with ESH subject to 4-point bending. Figure 2 shows the schematic drawing of this test. The moment capacity of CFSCB with ESH was investigated with various hole sizes and hole spacings. In total, 12 specimens were tested which included channels with both edge-stiffened and un-stiffened holes. The test results of Chen et al. [8] were utilized in this study to validate the FE models developed herein.

3. Summary of finite element results reported by Dai et al. [25]

3.1 Material properties

ABAQUS [26] was used to develop nonlinear elasto-plastic FE models to obtain the moment capacity of CFSCB with ESH. The measured section dimensions and material parameters obtained from the tensile coupon tests [8] were used to develop FE models.

3.2 Element type and mesh size

The FE models of CFSCB were developed using S4R shell elements. Based on the results of the mesh sensitivity analysis, a 5 mm×5 mm mesh size (width by length) was chosen.

3.3 Boundary conditions and loading procedure

In the FE models, "Surface-to-surface" interaction was applied to simulate the contacts between CFSCB webs and load-transfer blocks, and "Hard contact" in the normal direction was set to prevent any possible penetration between the two surfaces. The screws and bolts were

simulated utilising multi-point constraint beam connectors. The boundary condition of the end roller supports was simulated through the release of in-plane rotation and displacement in the direction of the beam length. The "Static General" analysis type was set for the simulation of bending tests in ABAQUS [25]. The large displacements of elements were simulated in the FE analysis by activating the "*NLGEOM" option in ABAQUS. Figure 3 shows more details of the boundary and loading conditions used in the FE model for W240-L4-EH3. The label "W240-L4-EH3" means the web depth, length and the number of edge-stiffened holes as 240 mm, 4 m and 3, respectively. Similar FE modelling techniques for CFS beams were reported in [25, 27].

3.4 Modelling of initial geometric imperfections

In the FE models, initial geometric imperfections were considered. Local and lateral-torsional geometric imperfections were taken into consideration. For each CFSCB with ESH, a buckling analysis was performed to obtain the eigenvalues and eigenmodes, and the lowest eigenmode was applied to each model. The magnitudes of local and lateral-torsional imperfections of CFSCB with ESH were scaled to the values obtained from the tests for validation purpose and then for the other FE models, the magnitudes of imperfections were taken from the recommendations of AS/NZS (2018) [6].

3.5 Validation of FE models

The moment capacities obtained from the FEA were compared with the test data reported by Chen et al. [8]. Table 1 shows the comparison results. The eigen values are presented in Table 1. The value of the ratio of the test to FEA moment capacities (M_{TEST}/M_{FEA}) is 1.01 on average, and the coefficient of variation (COVs) is 0.03. It can be seen from Table 1 that the FEA results are quite close to the test data. The deformed shapes of the sections, as obtained from the FEA, are shown in Figure 4, and they match closely with the experimentally obtained failure modes.

4. eXtreme Gradient Boosting (XGBoost) machine learning tool

4.1 Overview

XGBoost (eXtreme Gradient Boosting) is a collection of algorithms that is built on the Boosting framework, and is extremely powerful in terms of parallelism, missing value handling, and predictive performance analysis. XGBoost has a number of advantages including supporting efficient parallel training, fast training speed, low memory usage, high reliability, and widespread support. XGBoost optimizes the algorithm robustness. The treatment of missing values is determined by enumerating if each missing value is stored in the left or right subtree at the present node. The approach contains L1 and L2 regularisation terms to avoid overfitting and has a greater capacity for generalisation. L1 and L2 regularisation terms have different effects on weights; Weights are encouraged to be small by L2 regularisation (controlled by the lambda term), whereas weights are encouraged to be zero by L1 regularization (controlled by the alpha term). This is beneficial in models such as logistic regression, which requires some feature selection.

4.2 Cross validation

During the training phase, the overfitting problem frequently occurs, which means that the training data can be well fitted. The original data are divided into K groups and a validation set is created for all subsets, while using the remainder of the K-1 subset data as the training set, in order to build the K models. The validation set is divided into K models, and the cross-validation error is calculated by summing and averaging the final mean squared error (MSE). Cross-validation makes efficient use of sparse data and ensures that the evaluation results are as near to the performance of the models on the test set as feasible.

4.3 Performance evaluation

To evaluate the performance of each prediction method, the absolute percentage error ($Err_i(\%)$), coefficient of determination (R2), mean absolute error (MAE), and the root mean square error (RMSE) were determined. The Equations (1)-(4) were used to determine each of these parameters:

$$\mathrm{Err}_i(\%) = \frac{|y_i - t_i|}{t_i} \times 100 \tag{1}$$

$$R^2 = \frac{\sum_{i=1}^{N}(y_i - \overline{y_i})(t_i - \overline{t_i})}{\sqrt{\sum_{i=1}^{N}(y_i - \overline{y_i})^2 \sum_{i=1}^{N}(t_i - \overline{t_i})^2}} \tag{2}$$

$$\mathrm{RMSE} = \sqrt{\frac{\sum_{i=1}^{N}(t_i - y_i)^2}{N}} \tag{3}$$

$$\mathrm{MAE} = \frac{\sum_{i=1}^{N}|y_i - t_i|}{N} \tag{4}$$

where, t_i and y_i represent the real and prediction output values for the subsequent output, respectively, and $\overline{t_i}$ and $\overline{y_i}$ represent the averages of the real and predicted outputs, respectively. *N* represents the data series.

4.4 Data training for the moment capacity prediction

To develop prediction models for the moment capacity of CFSCB with ESH, the data obtained from validated FE

models were utilized. Prior to normalisation, the XGBoost's input and output data points were formulated as Equations (5) and (6):

$$\text{Input} = \{b_w, t, a, q, s, L\} \quad (5)$$

$$\text{Output} = \{P_{\text{out}}\} \quad (6)$$

The data was split into two groups: training data and testing data. A total of 1620 data vectors were utilized for this investigation. The database was randomly split into the training set and testing set with the ratio of 70% and 30%, respectively.

4.5 Performance measure of the developed model

The performance of the XGBoost model was evaluated in accordance with R^2, RMSE, and MAE. The value of R^2 represents the accuracy with which the proposed formulation can anticipate the data. The RMSE is referred to as the cost function. Both RMSE and MAE were used to evaluate the accuracy and quality of fit. A good predictor model has a lower RMSE and MAE and is closer to that with an R^2 value of 1.00. The performance metrics for training and testing sets were both determined utilising a training-testing split with a 70%-30% ratio of the entire database.

A model with a high R^2 value and a low error is deemed to have a high statistical performance. As shown in Table 2, the R^2 value determined by the training set is the highest (0.9999955), while the MAE and RMSE values are 0.0087001 and 0.0132404, respectively. In the XGBoost model, the R^2, RMSE, and MAE values for the testing set are 0.9998403, 0.0829422 and 0.0459597, respectively.

The performance of XGBoost model was also checked by comparing its results with the results obtained from the Linear Regression model. As shown in Tables 2 and 3, XGBoost outperforms the prediction of the Linear Regression model by a wide margin.

4.6 Comparison of machine-learning testing datasets with design strengths

The moment capacities obtained from the XGBoost testing dataset were also compared with that determined from the existing design equations proposed by Moen and Schafer [28, 29] and Yu [7]. The moment capacities determined from the design equations for USH [28, 29] and ESH [7] were found to be excessively conservative by 38.3%, and unconservative by 36.2% on average, respectively.

4.7 Comparison of machine-learning predictions with the current design strengths

As shown Table 4, the absolute error in percentage for moment capacities of CFSCB with ESH determined by the XGBoost model, Moen and Schafer equations [28, 29] and Yu equations [7] are 6.61%, 35.26%, and 42.15%, respectively. It can be found that the moment capacities of CFSCB with ESH determined by the equations proposed by Moen and Schafer [28, 29] and Yu [7] are much lower than the XGBoost predictions. Compared with the design strengths mentioned above, the XGBoost results have the best performance in predicting the moment capacity of CFSCB with ESH.

5. Proposed design equations

As mentioned before, only Yu [7] proposed design equations for the prediction of moment capacity of CFSCB with ESH. Nevertheless, no test data was used for the validation of Yu's equation and more importantly his equation was only for columns failing in local buckling and did not include other failure modes such as distortional buckling and lateral-torsional buckling. In addition, the validated XGBoost model predicted the moment capacity of CFSCB with ESH with a higher degree of precision as compared to the existing design equations. Therefore, the results derived from the XGBoost model were used to propose new design equations for predicting the moment capacity of CFSCB with ESH.

5.1 Proposed equations for CFSCB with ESH

For lateral-torsional buckling failure, the moment capacity of CFSCB with ESH can be calculated using Equations (7)-(9).

When $M_{\text{op}} < 0.573M_{\text{y}}$, $M_{\text{bep}} = 1.7M_{\text{op}}$ (7)

When $0.573M_{\text{y}} \le M_{\text{op}} \le 1.25M_{\text{y}}$, $M_{\text{bep}} = 2M_{\text{op}} - 0.5M_{\text{y}}$ (8)

For $1.25M_{\text{y}} < M_{\text{op}}$, $M_{\text{bep}} = 1.9M_{\text{op}} - 1.44M_{\text{y}}$ (9)

where, M_{op} is the critical elastic lateral-torsional buckling moment of CFSCB; M_{y} is the member yield moment of the gross section; and M_{bep} is the proposed nominal member moment capacity for lateral-torsional buckling of CFSCB with ESH.

For local buckling failure, the moment capacity of CFSCB with ESH can be calculated using the following Equations (10)-(11).

For $\lambda_{\text{l}} \le 0.439$, $M_{\text{blp}} = 1.7M_{\text{op}}$ (10)

For $\lambda_{\text{l}} > 0.439$, $M_{\text{blp}} = [1 - 0.15(\frac{M_{\text{olp}}}{M_{\text{op}}})^{0.75}](\frac{M_{\text{olp}}}{M_{\text{op}}})^{0.75} M_{\text{y}}$ (11)

where, M_{blp} is the proposed nominal member moment capacity for local buckling, and M_{olp} is the elastic local buckling moment capacity of CFSCB.

For distortional buckling failure, the moment capacity of CFSCB with ESH can be calculated using Equations (12)-(13).

For $\lambda_d \leq 0.873$, $M_{bdp} = M_y$ (12)

For $\lambda_d > 0.873$, $M_{bdp} = [1.25 - 0.33(\frac{M_y}{M_{odp}})^{0.5}]M_y$ (13)

where, M_{bdp} is the proposed nominal member moment capacity for local buckling failure of CFSCB with ESH, and Modp is the elastic local buckling moment capacity of CFSCB.

5.2 Reliability analysis

A reliability analysis was undertaken to evaluate the performance of proposed design equations for calculating the moment capacity of CFSCB with ESH. Any proposed design equation is accounted as reliable if its reliability index (β') is not less than 2.50, as per the guidelines of AISI [5]. Equation (14) (as given below) [5] was used to calculate the reliability indices of the proposed design equations. In Equation 40, the values of M_m and V_m were taken as 1.1 and 0.1, respectively, which were determined by the mean and COV values of the material factor. The values of F_m and V_f were 1.0 and 0.05, respectively, which were determined from the mean and COV values of the fabrication factor. The value of Vq was set 0.21 which again was determined by the COV value of the load factor. Cp represents the correction factor. As shown in Table 5, the reliability indices of all the proposed equations are greater than 2.5, which confirms that the proposed design equations can accurately predict the moment capacity of CFSCB with ESH and USH subject to bending.

$$\varphi = CM_m F_m P_m \exp(-\beta' \sqrt{V_m^2 + V_f^2 + C_p V_p^2 + V_q^2}) \quad (14)$$

6. Conclusions

The moment capacity of CFSCB with ESH subject to bending was predicted using a novel machine learning model which was developed using the XGBoost tool. Prior to the development of the machine learning model, nonlinear elasto-plastic FE models were developed and validated against the test results available in the literature. To train the XGBoost model, a total of 1,620 data points were generated from the validated FE models. The R^2 score of XGBoost predictions for the moment capacity of CFSCB with ESH was found to be around 99%.

The moment capacities obtained from the XGBoost testing dataset were also compared with that determined from the existing design equations proposed by Moen and Schafer for USH, and Yu for ESH. These equations were used to calculate the strengths of CFSCB with USH and ESH, respectively. The moment capacities determined from the design equations for USH and ESH were found to be excessively conservative by 38.3% on average, and unconservative by 36.2% on average, respectively. Then a total of ten dimensions were randomly selected for the moment capacity comparison using XGBoost, Moen and Schafer equations, and Yu equations. The absolute errors in percentage for moment capacities of CFSCB with ESH determined by the XGBoost model, Moen and Schafer equations and Yu equations were 6.61%, 35.26%, and 42.15%, respectively.

As the existing design rules were not capable of accurately predicting the moment capacity of CFSCB with ESH, the results of the XGBoost machine learning prediction were utilized to propose new design equations for predicting the moment capacity of such beams. The mean value of the absolute error in percentage for the proposed design equations of CFSCB with ESH based on the strengths of unperforated CFSCB is 8.78%. Additionally, a reliability analysis was conducted to demonstrate that the proposed design equations are reliable and can accurately predict the moment capacity of cold-formed steel channel beams with edge-stiffened and un-stiffened web holes.

References

[1] J. Ye, G. Quan, P. Kyvelou, L. Teh, L. Gardner. A practical numerical model for thin-walled steel connections and built-up members, Struct. 38 (2022) 753-764.

[2] J. Ye, G. Quan, X. Yun, X. Guo, J. Chen. An improved and robust finite element model for simulation of thin-walled steel bolted connections, Eng. Struct. 250 (2022) 113368.

[3] H.T. Li, B. Young, Design of cold-formed high strength steel tubular sections undergoing web crippling, Thin-Walled Struct. 133 (2018) 192-205.

[4] Howick Floor, Joist System. (2013) Auckland, New Zealand.

[5] American Iron and Steel Institute (AISI), North American Specification for the Design of Cold-formed Steel Structural Members AISI S100-16, 2016.

[6] Australia/New Zealand Standard (AS/NZS), Cold-Formed Steel Structures, AS/NZS 4600:2018. Standards Australia/ Standards New Zealand, 2018.

[7] Cold-formed steel flexural member with edge stiffened holes: Behavior, optimization, and design, J. Constr. Steel Res. 71 (2012) 210-218.

[8] Moment capacity of cold-formed channel beams with edge-stiffened web holes, un-stiffened web holes and plain webs, Thin-Walled Struct. 2020. 157 (2020) 107070. https://doi.org/10.1016/j.tws.2020.107070.

[9] B. Chen, K. Roy, Z. Fang, A. Uzzaman, G.M. Raftery, J.B.P. Lim, Moment capacity of back-to-back cold-formed steel channels with edge-stiffened holes, un-stiffened holes, and plain webs, Eng. Struct. 235 (2021) 112042.
[10] B. Chen, K. Roy, A. Uzzaman, G.M. Raftery, D. Nash, G.C. Clifton, P. Pouladi, J.B.P. Lim, Effects of edge-stiffened web openings on the behaviour of cold-formed steel channel sections under compression, Thin-Walled Struct. 144 (2019) 106307.
[11] B. Chen, K. Roy, A. Uzzaman, G.M. Raftery, J.B.P. Lim, Parametric study and simplified design equations for cold-formed steel channels with edge-stiffened holes under axial compression, J. Constr. Steel Res. 172 (2020) 106161.
[12] B. Chen, K. Roy, A. Uzzaman, G.M. Raftery, J.B.P. Lim, Axial strength of back-to-back cold-formed steel channels with edge-stiffened holes, un-stiffened holes and plain webs, J. Constr. Steel Res. 174 (2020) 106313.
[13] Y. Chi, K. Roy, B. Chen, Z. Fang, A. Uzzaman, G.B.G. Ananthi, J.B.P. Lim, Effect of web hole spacing on axial capacity of back-to-back cold-formed steel channels with edge-stiffened holes, Steel Compos. Struct. 40 (2021) 287-305.
[14] Z. Fang, K. Roy, B. Chen, C.W. Sham, I. Hajirasouliha, J.B.P. Lim, Deep learning-based procedure for structural design of cold-formed steel channel sections with edge-stiffened and un-stiffened holes under axial compression, Thin-Walled Struct. 166 (2021) 108076.
[15] A. Uzzaman, J.B.P. Lim, D. Nash, B. Young, Effects of edge-stiffened circular holes on the web crippling strength of cold-formed steel channel sections under one-flange loading conditions, Eng. Struct. 139 (2017) 96-107.
[16] A. Uzzaman, J.B.P. Lim, D. Nash, K. Roy, Cold-formed steel channel sections under end-two-flange loading condition: Design for edge-stiffened holes, unstiffened holes and plain webs, Thin-Walled Struct. 147 (2020) 106532.
[17] A. Uzzaman, J.B.P. Lim, D. Nash, K. Roy, Web crippling behaviour of cold-formed steel channel sections with edge-stiffened and unstiffened circular holes under interior-two-flange loading condition, Thin-Walled Struct. 154 (2020) 106813.
[18] B. Chen, K. Roy, Z. Fang, A. Uzzaman, Y. Chi, J.B.P. Lim, Web crippling capacity of fastened cold-formed steel channels with edge-stiffened web holes, un-stiffened web holes and plain webs under two-flange loading, Thin-Walled Struct. 163 (2021) 107666.
[19] B. Chen, K. Roy, Z. Fang, A. Uzzaman, C.H. Phan, G.M. Raftery, J.B.P. Lim, Shear capacity of cold-Formed steel channels with edge-stiffened web holes, unstiffened web Holes, and plain webs, J. Struct. Eng. ASCE 148(2) (2022) 04021268.
[20] E. Kanthasamy, K. Thirunavukkarasu, K. Poologanathan, P. Gatheeshgar, S. Todhunter, T. Suntharalingam, M.F.M. Ishqy, Shear behaviour of doubly symmetric rectangular hollow flange beam with circular edge-stiffened openings, Eng. Struct. 250 (2022) 113366.
[21] J. Rahman, K.S. Ahmed, N.I. Khan, K. Islam, S. Mangalathu, Data-driven shear strength prediction of steel fiber reinforced concrete beams using machine learning approach, Eng. Struct. 233 (2021) 111743.
[22] M.A.B. Kabir, A.S. Hasan, A.M. Billah, Failure mode identification of column base plate connection using data-driven machine learning techniques, Eng. Struct. 240 (2021) 112389. https://doi.org/10.1016/j.engstruct.2021.112389.
[23] T. Chen, C. Guestrin, XGBoost: A scalable tree boosting system, the 22nd ACM SIGKDD International Conference ACM (2016).
[24] V.V. Degtyarev, K.D. Tsavdaridis, Buckling and ultimate load prediction models for perforated steel beams using machine learning algorithms, J. Build. Eng. 51 (2022) 104316.
[25] Y. Dai, K. Roy, Z. Fang, B. Chen, G.M. Raftery, J.B.P. Lim, A novel machine learning model to predict the moment capacity of cold-formed steel channel beams with edge-stiffened and un-stiffened web holes, J. Build. Eng. 53 (2022) 104592.
[26] ABAQUS Analysis User's Manual-Version 6.14-2, ABAQUS Inc., USA, 2018.
[27] Z. Fang, K. Roy, Y. Dai, J.B.P. Lim, Effect of web perforations on end-two-flange web crippling behaviour of roll-formed aluminium alloy unlipped channels through experimental test, numerical simulation and deep learning, Thin-Walled Struct. 179 (2022) 109489.
[28] C.D. Moen, B.W. Schafer, Elastic buckling of cold-formed steel columns and beams with holes, Eng. Struct. 31(12) (2009) 2812-2824. https://doi.org/10.1016/j.engstruct.2009.07.007.
[29] C.D. Moen, A. Schudlich, and A.V.D. Heyden, Experiments on cold-formed steel C-section joists with unstiffened web holes, J. Struct. Eng. ASCE 139(5) (2013) 695-704. https://doi.org/10.1061/(ASCE)ST.1943-541X.0000652.

Figure 1: CFSCB as the primary load-carrying members [8]

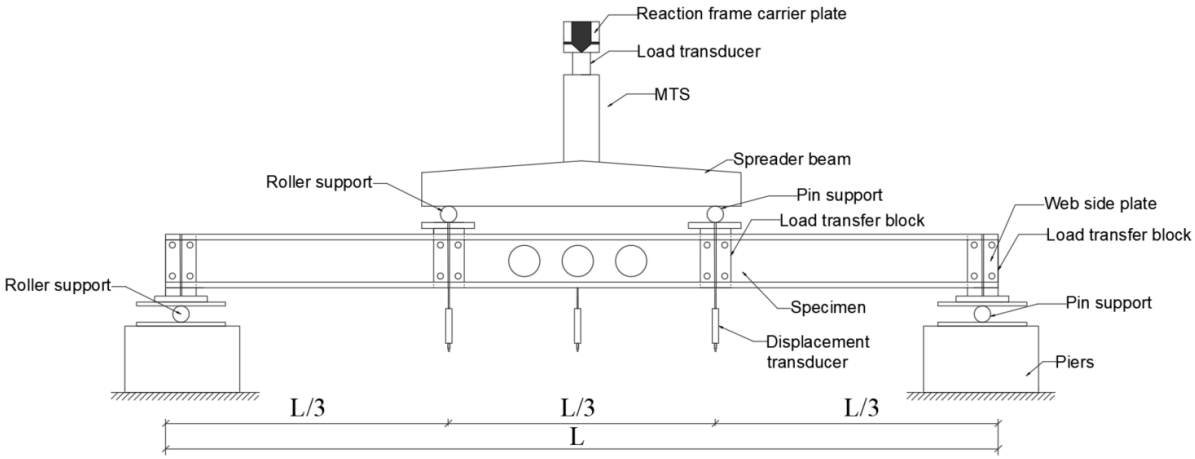

Figure 2: Schematic drawing of 4-point bending tests conducted by Chen et al. [8]

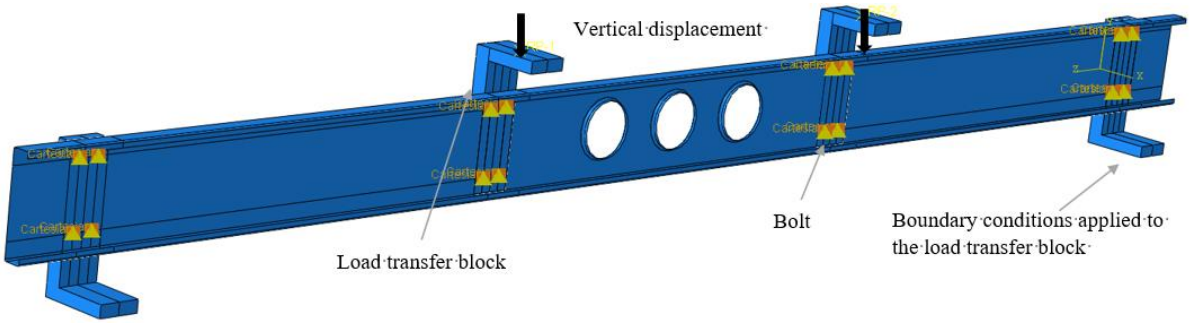

Figure 3: Boundary condition applied to the FE model of W240-L4-EH3 [25]

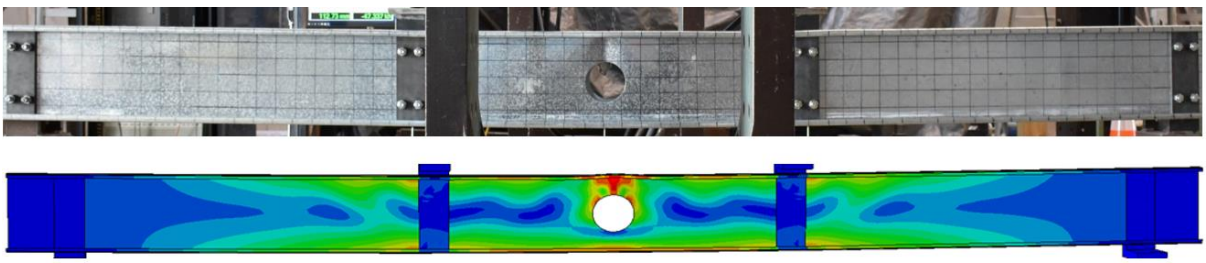

Figure 4: Deformed shapes at failure from experiments [8] and FEA (W290-L4-UH1) [25]

Table 1: Moment capacity of CFSCB obtained from the tests [8] and FEA [25]

Specimen	Web depth b_w (mm)	Thickness t (mm)	Hole spacing s (mm)	Moment capacity of tests [8] M_{TEST} (kN·m)	Moment capacity of FEA M_{FEA} (kN·m)	Eigen value	M_{TEST} / M_{FEA}
CFSCB with ESH							
W240-L4-EH1	240.8	1.85	-	12.9	12.97	7326	0.99
W240-L4-EH3	240.2	1.80	100	13.3	13.39	7639	0.99
W240-L4-EH5	240.6	1.81	50	13.7	13.93	7722	0.98
W290-L4-EH1	290.8	2.13	-	19.3	18.31	8408	1.05
W290-L4-EH3	290.3	2.15	100	19.8	19.12	8655	1.04
W290-L4-EH5	291.2	2.10	50	20.5	19.98	8635	1.03
CFSCB with USH							
W240-L4-UH1	241.6	1.82	-	11.0	11.75	6643	0.94
W240-L4-UH3	239.8	1.80	100	10.6	10.85	6853	0.98
W240-L4-UH5	239.6	1.81	50	10.2	10.17	6645	1.00
W290-L4-UH1	290.9	2.16	-	16.7	16.75	7353	1.00
W290-L4-UH3	290.0	2.11	100	16.3	15.46	7470	1.05
W290-L4-UH5	290.5	2.10	50	15.7	15.19	7348	1.03
Mean							1.01
COV							0.03

Table 2: The performance measure of XGBoost model [25]

XGBoost Training			XGBoost Testing		
R^2	RMSE	MAE	R^2	RMSE	MAE
0.9999955	0.0132404	0.0087001	0.9998403	0.0829422	0.0459597

Table 3: The performance measure of Linear Regression model [25]

Linear Regression Training			Linear Regression Testing		
R^2	RMSE	MAE	R^2	RMSE	MAE
0.9016	1.9904	1.5166	0.8943	4.2239	1.5967

Table 4: Absolute percentage errors for the prediction of moment capacities for CFSCB with ESH [25]

Specimen ID	Moment capacity (kN·m)	Err% (Moen and Schafer [31, 32])	Err% (Yu [12])	Err% (XGBoost)
1 W290-L4-EH1	19.30	22.80	3.08	10.26
2 W290-L4-EH3	19.80	25.76	0.47	9.29
3 W290-L4-EH5	20.50	29.27	2.96	10.93
4 W240-L5-EH4	12.39	17.28	7.12	6.97
5 W290-L6-EH2	15.82	26.67	25.77	4.50
6 W240-L7-EH1	10.04	37.93	32.24	0.84
7 W290-L8-EH5	12.43	42.54	60.10	5.24
8 W240-L9-EH2	7.60	49.09	74.61	3.30
9 W240-L10-EH4	6.59	51.76	101.34	10.76
10 W290-L10-EH5	9.30	49.49	113.80	4.01
Mean		35.26	42.15	6.61
COV		0.35	1.01	0.53

Table 5: Comparison of FEA strengths and proposed design strengths for CFSCB with ESH [25]

(a) For lateral-tortional buckling

Non-dimensional slenderness	$M_o < 0.573M_y$	$0.573M_y \le M_o \le 1.25M_y$	$1.25M_y < M_o$
Ratio of equations	M_{FEA} / M_{prop}	M_{FEA} / M_{prop}	M_{FEA} / M_{prop}
Data number	972	297	216
Mean, P_m	1.203	1.218	0.998
COV	0.104	0.075	0.029
β' [18]	3.3	3.5	2.81
φ [18]	0.85	0.85	0.85

(b) For local buckling

Non-dimensional slenderness	$\lambda_l \le 0.439$	$\lambda_l > 0.439$
Ratio of equations	M_{FEA} / M_{prop}	M_{FEA} / M_{prop}
Data number	972	513
Mean, P_m	1.198	1.007
COV	0.105	0.129
β' [18]	3.29	2.53
φ [18]	0.85	0.85

(c) For distortional buckling

Non-dimensional slenderness	$\lambda_d \le 0.873$	$\lambda_d > 0.873$
Ratio of equations	M_{FEA} / M_{prop}	M_{FEA} / M_{prop}
Data number	27	54
Mean, P_m	0.957	1.007
COV	0.008	0.027
β' [18]	2.66	2.85
φ [18]	0.85	0.85